UDK 620.17:620.193:620.3:544.1:661.666
Original scientific article/Izvirni znanstveni članek

ISSN 1580-2949
MTAEC9, 55(3)401(2021)

MODIFYING GO AND DOPING IT IN WATERBORNE ACRYLIC COATINGS TO ENHANCE THEIR MECHANICAL PERFORMANCE AND CORROSION PROTECTION

IZBOLJŠANJE MEHANSKIH IN ANTIKOROZIJSKIH LASTNOSTI GRAFEN-OKSIDA Z NJEGOVO MODIFIKACIJO IN DOPIRANJEM V VODNI SUSPENZIJI NASTALE AKRILNE PREVLEKE

Xiao Wang[1], Yixiao Xie[2], Weiwei Cong[1], Zhaolei Li[2], Zexiao Xu[3], Hui Yan[4], Taijiang Gui[1*], Weili Li[2*]

[1]State Key Laboratory of Marine Coatings, Marine Chemical Research Institute Co., Ltd., Qingdao 266071, China
[2]School of Material Science and Engineering, Jiangsu University of Science and Technology, Zhenjiang 212003, China
[3]Suzhou Jiren Hi-Tech Material Co., Ltd, Suzhou 215143, P. R. China
[4]Department of Chemistry, University of Louisiana at Lafayette, Lafayette, LA 70504, USA

Prejem rokopisa – received: 2020-12-31; sprejem za objavo – accepted for publication: 2021-03-12

doi:10.17222/mit.2021.010

With the ever-increasing focus on environmental protection, the waterborne acrylic resin-based coating has been commonly used in a wide range of applications due to its flexibility and good UV resistance. Continuous attempts have been extensively carried out to improve its corrosion resistance and mechanical properties through the doping of different nanomaterials. In this study, Functionalized Graphene Oxide (FGO) nanosheets covalently bonded to hydroxylated acrylic resins were introduced into the Hydroxyacrylic Acid Dispersion (HAD) matrix to enhance the performance. To study the effect of grafted hydroxylated acrylic resin on the morphology and properties of GO nanosheets, the GO and FGO nanosheets were systematically characterized with various testing methods, such as FTIR and field-emission scanning electron microscopy (FE-SEM), transmission electron microscopy (TEM), Raman spectroscopy, X-ray diffraction (XRD) analysis, UV–vis analysis, and thermogravimetric analysis (TGA). The morphology, physical-mechanical, and anti-corrosion properties of the HAD coatings doped with GO and FGO nanosheets were compared. The results confirmed that FGO's dispersion behavior in the HAD matrix was improved after modification with the hydroxylated acrylic resin, and the interfacial bonds between the HAD-FGO nanosheets were significantly enhanced.

Keywords: hydroxyacrylic acid dispersion coating, modified graphene oxide, grafting, mechanical properties, anti-corrosion properties

Razvoj znanosti in tehnologije ter vedno večji pomen zaščite okolja na področju v vodi nastajajočih akrilnih prevlek omogoča, zaradi fleksibilnosti in dobre odpornosti pred ultravijoličnim sevanjem (UV), njihovo uporabo na mnogih področjih. Znanstveniki in raziskovalci poizkušajo stalno izboljšati njihovo korozijsko odpornost in mehanske lastnosti s pomočjo dopiranja z različnimi nano-materiali. Avtorji v pričujočem članku opisujejo izboljšanje lastnosti prevlek z vpeljavo nano ploščic funkcionaliziranega grafen oksida (FGO), kovalentno vezanega s hidroksilatno akrilnimi smolami, v matrico kisle hidroksiakrilne disperzije (HAD). S pomočjo različnih metod karakterizacije, kot so: Furierjeva transformacijska infrardeča spektroskopija (FTIR), vrstična elektronska mikroskopija, mikroskopija na emisijo polja (FE-SEM), presevna elektronska mikroskopija (TEM), Raman-ova spektroskopija, rentgenska difrakcija (XRD), UV–vis analiza in termogravimetrija (TGA), so študirali vpliv cepljene hidroksilirane akrilne smole na morfologijo in lastnosti GO ter GO in FGO nanoploščic. Med seboj so primerjali morfologijo, fizikalno-mehanske in antikorozijske lastnosti HAD prevlek dopiranih z GO in FGO nanoploščicami. Rezultati raziskav so pokazali, da se je disperzijsko obnašanje FGO v HAD matrici izboljšalo po modifikaciji s hidroksilirano akrilno smolo, prav tako pa se je občutno izboljšala povezava na mejah med HAD in FGO nanoploščicami.

Ključne besede: v kislini dispergirana hidroksiakrilna prevleka, modificirani grafen oksid, cepljenje, mehanske in antikorozijske lastnosti

1 INTRODUCTION

Organic coatings have been widely used to protect metals against corrosion by functioning as a physical barrier between the metal surface and the corrosive environment.[1] In recent years, with the increased concern about environmental pollution, waterborne polymer painting is begining to attract people's attention. Among them, acrylic resin is thought to be one of the most attractive polymer materials due to its excellent adhesive, flexibility, and weather resistant properties.[2–4] However, for a coating based on waterborne acrylic resin, its hydrophilic nature can degrade the performance of the coating's barrier, because the corrosive species such as oxygen, water, and chloride ions can reach the metal/coating interface through diffusion into the coating porosities.[5] To make things even worse, the corrosion of metal beneath the coating can accelerate the loss of adhesion and the blistering of the coating simultaneously. Thus, its mechanical and anti-corrosion properties still need to be improved when compared with the traditional solvent-organic coatings.[6]

*Corresponding author's e-mail:
tjgui@163.com (Taijiang Gui)

Recently, with unique structural and physical properties, graphene or graphene oxide nanosheets have attracted interest due to the 2D structure's single layer of carbon atoms.[7,8] It is a promising nanomaterial in the field of anti-corrosion due to its outstanding chemical stability, high specific surface area, and superior barrier properties. The doping of these nanomaterials into a polymer matrix provides exceptional mechanical properties and multi-functional characteristics, which have been proposed as a better alternative to the traditional carbon nanotube (CNT).[9–11] For example, Ken-Hsuan Lia et al. showed that functionalized GO can be uniformly dispersed in a thermosetting polyurethane acrylate and enhance the properties of cured composites.[12] Ling Hu uniformly dispersed modified amine-GO nano-tablets in Waterborne Polyurethane (WPU), which led to an improvement in the glass transition temperature, tensile strength, and hydrophobicity of the cured WPU coating.[13] Xiaogang Li et al. prepared novel aniline trimer functionalized graphene sheets (SAT-G) using the intercalation and silanization of trianiline precursor. The as-prepared SAT-G hybrid displayed good dispersion in epoxy resin, which was available for filling the defects in the epoxy matrix and then significantly prevent the permeation of aggressive medium from the coating.[14]

Although graphene or graphene oxide presents very promising properties, the strong interlayer force between the adjacent graphene sheets easily leads to their agglomeration in a polymer matrix.[15,16] To optimize the dispersion behavior of graphene or graphene oxide and strengthen their interfacial interaction with polymer matrix, a chemical or physical modification of graphene is needed.[17–20] In this paper, GO was first modified with low-molecular-weight hydroxyl acrylic resin via a dehydration reaction, after which the obtained functional GO (FGO) was doped into the hydroxy acrylic acid dispersion (HAD) by in-situ polymerization. To effectively improve the interface between the FGO nanosheets andt he HAD, the effect of FGO on the morphology and properties of the dried HAD coatings was studied.

2. EXPERIMENTAL

2.1 Materials

Squama graphite was purchased from Suzhou Hengqiu Technologies. Concentrated sulfuric acid (H_2SO_4, 98 %), hydrochloric acid (HCl), N, N-dimethyl ethanolamine, and hydrogen peroxide(H_2O_2, 30 *w*/%) were purchased from Sinopharm Chemical Reagent Co. Ltd. Potassium permanganate ($KMnO_4$, A. R.) and sodium nitrate ($NaNO_3$, A. R.) were supplied by Shanghai Su Yi Chemical Reagent Co. Ltd. The monomers, such as methylmethacrylate (MMA, C. P.), ethylhexyl acrylate (2-EHA, C. P.), hydroxyethyl acrylate (HEA, C. P.), isobornyl methacrylate (IBOMA, C. P.), and acrylic acid (AA, C. P.) were purchased from Shanghai Sepal Chemical Factory Co., Ltd. Di-Tert-Butyl peroxide (DTBP, JiangSu Quan Wei Polymer Materials Co., Ltd) Glycidyl tertiary carbonate (E10P) was obtained from Momentive Co., Ltd. THF (A. R.), DMF (A. R.) and dipropylene glycol mono-n-butyl ether (DPNB) were used without purification and were purchased from Shanghai Titanchem Co. Ltd., dicyclohexylcarbodiimide(DCC) was purchased from Zhanwang Chemical Reagent Co. Ltd. Isocyanate curing agent, Aquolin®268, Wanhua Chemical Group Co., Ltd.

2.2 Preparation of functional GO (FGO)

First, graphite oxide (GO) was prepared from flaky graphite powders using a modified Hummers method.[21,22] Second, when MMA, 2-EHA, HEA were used as the comonomers, BPO as the thermal initiator, and DMF as the solvent, the low-molecular-weight hydroxyl acrylic resin (named L-HAR) (Hydroxyl Content: 4.2 %, M_n = 10400, M_w = 33280, PDI = 3.2) was synthesized by solution polymerization at a T_g of 0 °C. Third, L-HAR was grafted onto a GO nanosheet using DCC as the dehydrating agent. Then 0.5 g of GO was mixed with 50 mL of DMF under ultrasonication, followed by adding 5 g of L-HAR and 2 g of DCC. The resulting mixture was stirred at room temperature for 24 h under a N_2 atmosphere and was then washed by Di water and centrifuged

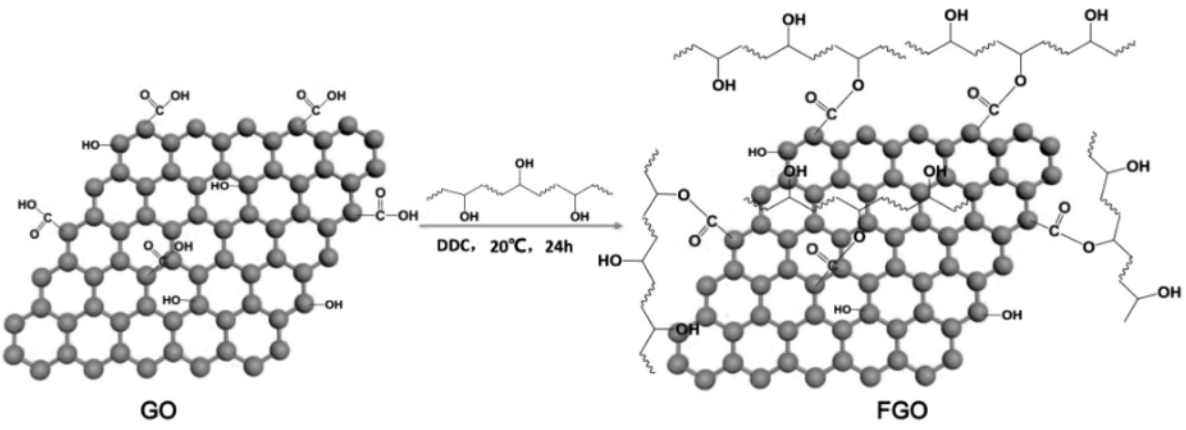

Figure 1: Schematic diagram of modifying GO with L-HAR

three times to remove the unreacted L-HAR, DCC, and the byproduct dicyclohexylurea(DCU). FGO was obtained after being dried under a vacuum.

Figure 1 presents the schematic diagram of the grafting reaction. As the L-HAR was grafted onto GO via chemical bonding, the dispersion behavior of FGO into polymer resins can be effectively improved.

2.3 In-situ preparation of hydroxyl acrylic dispersion

Glycidyl tertiary carbonate (E10P) and acrylic acid (AA) were added into a three-neck flask equipped with a stirrer, a thermometer, and a reflux condenser for 4–5 h at 160 °C.

When the acid value of the reaction system was reduced to 30 mg/g, DPNB and a certain amount of FGO were added at a lower temperature of 120 °C. After that, the mixture of acrylate monomers (MMA, 2-EHA, IBOMA, HEA) and the initiator DTBP were added dropwise for 4–5 h. The reaction was then kept for 1 h at 130 °C. Then the mixture was neutralized with triethanolamine and stirred for 2 h at 80 °C to obtain the FGO-doped hydroxyl acrylic dispersion, which is called FGO-d-HAD. The reaction mechanism is shown in **Figure 2**. The unmodified GO was also doped into the aqueous hydroxy acrylic acid dispersion using the same method (GO-d-HAD) as a reference.

2.4 Coating Procedure

Three sheets of steel panels (one for the mechanical test and two for the corrosion-resistance test) were polished using metallographic sandpaper first and then washed with alcohol to remove the dust. The waterborne isocyanate curing agent (Aquolin®268) was added to pure HAD, GO-d-HAD, or FGO-d-HAD. The mixture was coated onto the pre-treated substrates with an automatic coating machine (BGD 218). The dried coating was cured at room temperature for about 24 h, and the thickness of the dried coating was controlled to be around 100 μm.

2.5 Characterization

The morphologies and structures of the GO and FGO sheets were observed by transmission electron microscopy (TEM, PHILIPS Tecnai 12) and field-emission scanning electron microscopy (HITACHI S-4800 ¢ò FESEM), respectively. The samples were treated by lyophilization to maintain the morphology of the materials. For the TEM imaging, GO or FGO nanosheets were dispersed in ethanol by sonication for 15 min, and then transferred to carbon-coated copper grids. FTIR spectra were recorded on a Perkin-Elmer 16 PC FTIR spectrophotometer. The Raman spectra were measured with a Bruker Raman spectrometer (SENTERRA II, Germany) with a 514-nm laser excitation in the range 1000–2600 cm^{-1}. X-ray diffraction (XRD) was applied with a SHIMADZU XRD-6000 X-ray spectrometer with a Cu-K_α filament. UV–vis spectroscopy was conducted using a SHIMADZU UV3600. Thermogravimetric analyses (PE Pyris Diamond TG-DTA) were performed to investigate the thermal stability of the GO or FGO nanosheets, and the measurement was carried out in the temperature region 25–800 °C with a heating rate of 10 °C/min under nitrogen. Particle sizes and zeta-potential of the obtained composite (HAD, GO-d-HAD, and FGO-d-HAD) were measured on 90 Plus/B1-MAS Zeta plus ZetaPotential Analyzer, Brookhaven Instruments Corporation. The coating adhesion was tested by GFZ film adhesion tester according to GB/T 9286-1998. The coating toughness was tested by QTY-32 paint film bending tester according to GB/T 6742-2007. The coating hardness was tested by the QAQ paint film pencil hardness tester according to GB/T 6739-2006. The coating mechanical properties were tested by CMT-4304 electronic universal tensile testing machine of Shenzhen Xinsansi Material Testing Co., Ltd. according to GB/T 9286-1998, the tensile rate was 2 mm/min. In addition, the tensile fracture morphologies of the different coatings were observed with a scanning electron microscope (SEM, JSM-6480 JEOL Ltd). The corrosion resistance of the different coatings was characterized by Tafel polarization curves, and salt-spray tests, respectively. The first was carried out by the CS350H electrochemical working station. The second was operated by ywx/q-250 salt-spray corrosion-test chamber (Yangzhou hi-tech environmental test equipment Co., Ltd.) according to GB/T 1771-2007.

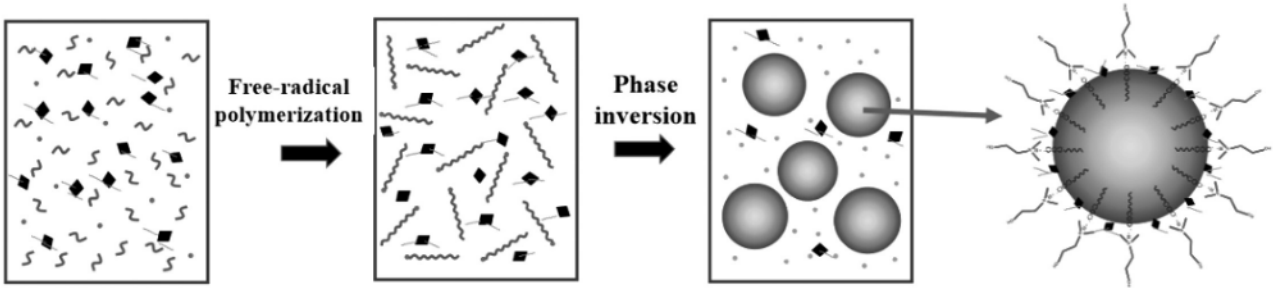

Figure 2: Schematic diagram of *in-situ* preparation of HAD doped with FGO

3 RESULTS AND DISCUSSION

3.1 Characterizations of GO and FGO nanosheets

Figure 3 presents the typical FT-IR spectra for GO and FGO. The main characteristic features are the absorption bands related to those stretching vibrations like C=O carbonyl and carboxylic groups at 1733 cm^{-1}, C-O-C stretching at 1151cm^{-1}, and C–O stretching at 1060 cm^{-1}. The peaks that appeared at 1632 cm^{-1} and 3410 cm^{-1} are attributed to the C=C and O-H stretching, respectively.[23] It should be noted that two absorption bands related to C-H bands are significantly enhanced for FGO at 2928 cm^{-1} and 2855 cm^{-1}, which indicates the L-HAR linkage with the GO surface. In addition, **Table 1** presents the intensity of the peaks that are normalized for that of the C=C bond. The decreased relative ratio of O-H/C=C and the increased relative ratios of C-H/C=C and C=O/C=C suggest that the reaction between the carboxylic groups of GO with hydroxyl groups of L-HAR[24] occurs. These results indicate that the L-HAR has interacted with hydroxyl groups of carboxylic groups on the GO sheets via a dehydration reaction.

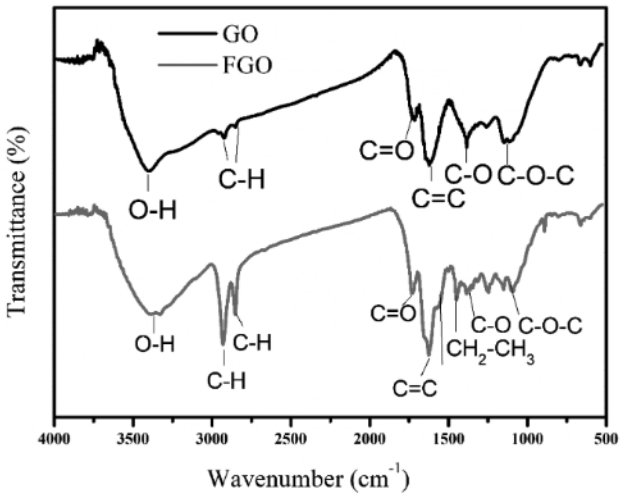

Figure 3: FT-IR spectra of GO and FGO nanosheets

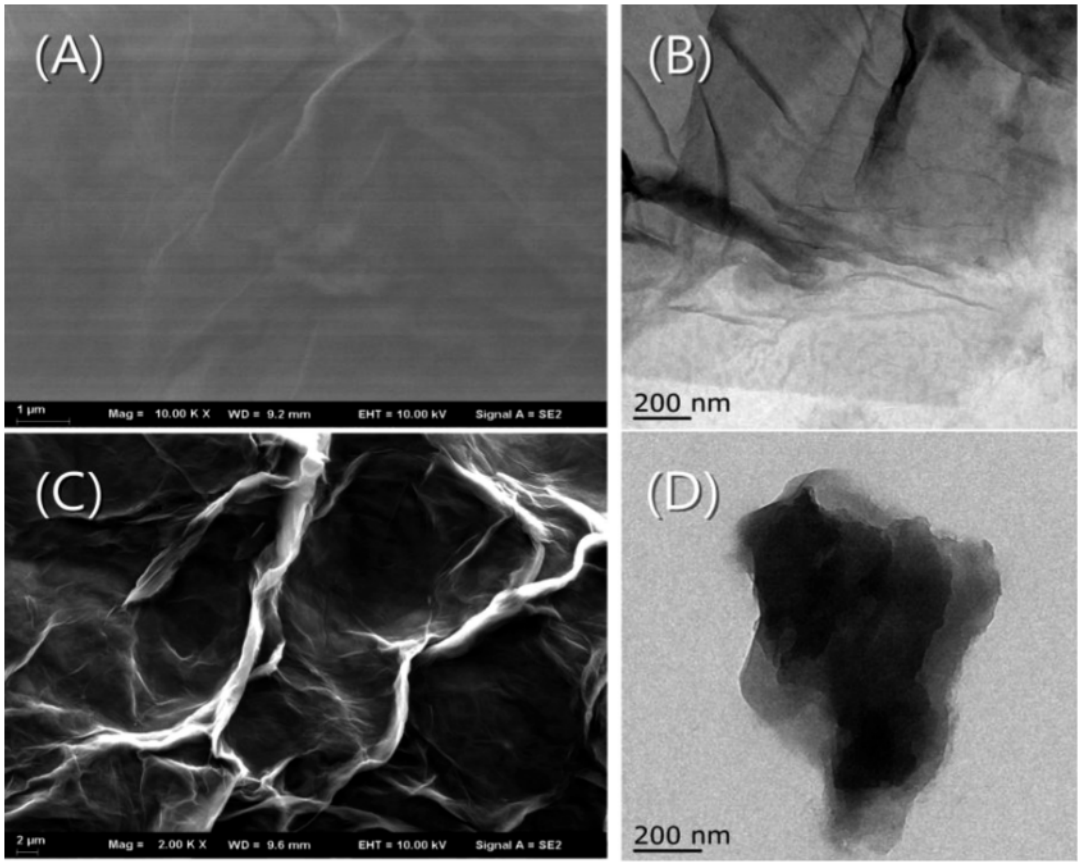

Figure 4: SEM and TEM images for GO a), b) and FGO c), d) nanosheets

Table 1: The ratios of relative intensities obtained from the FT-IR spectra of GO and FGO nanosheets

The ratio of the peaks	$\frac{O-H}{C=C}$	$\frac{C-H\ (2927\ cm^{-1})}{C=C}$	$\frac{C-H\ (2850\ cm^{-1})}{C=C}$	$\frac{C=O}{C=C}$
GO	1.03	0.78	0.70	0.61
FGO	0.72	0.93	0.73	0.635

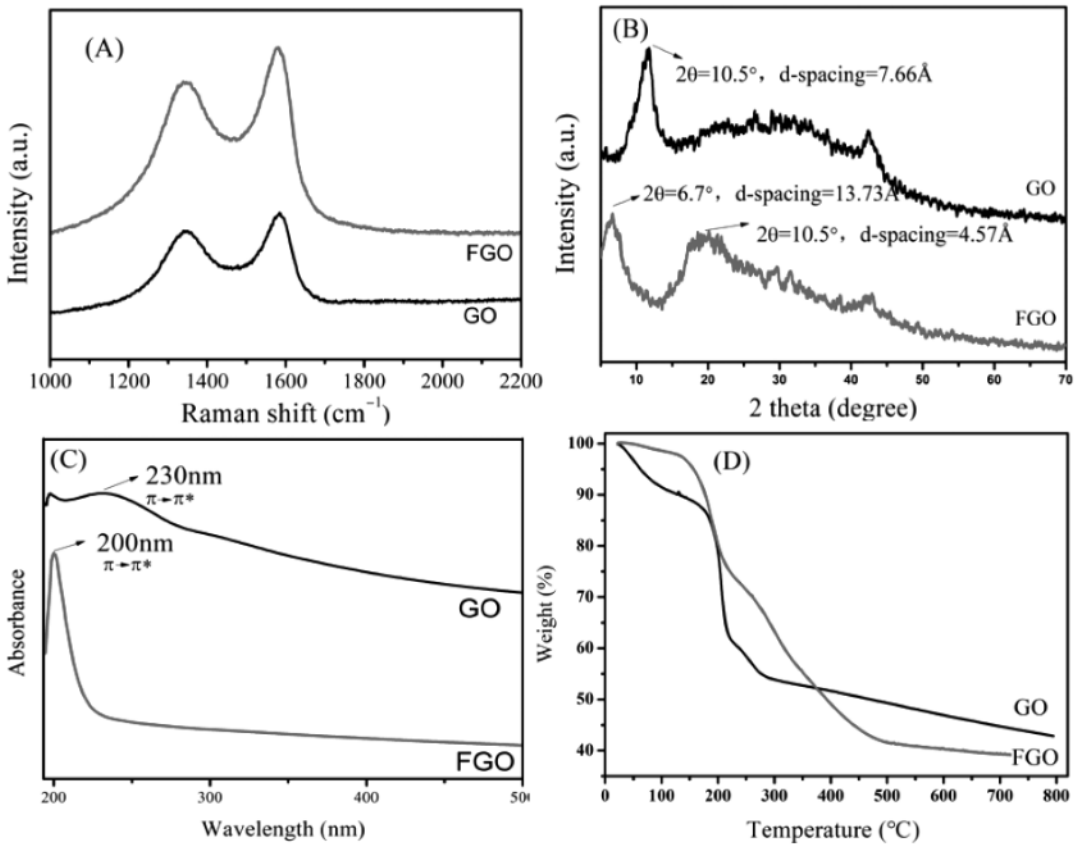

Figure 5: Characterizations of GO and FGO nanofillers: a) Raman spectra, b) XRD curves, c) UV-vis spectrum, and d) TGA curves

Figure 4 presents TEM and SEM images for the GO and FGO nanosheets. For pure GO, it shows a typically lucid and thin layer morphology. However, when it was grafted by L-HAR, the chemical-bond linking can lead to the stacking of GO, and the obtained FGO displays a folding and stacking morphology. The changes in morphology ban affect the properties of the FGO.

To explore the impact of the grafted L-HAR on the properties of GO, different measurements were applied and shown in **Figure 5**.

Two obvious peaks, D band at 1335 cm^{-1} and G band at 1581 cm^{-1} in the Raman spectra of GO and FGO, are shown in **Figure 5a**. They are ascribed to the structural defects and the first-order scattering of the E2g vibrational mode in the GO, respectively. The broadened G band implies a better exfoliation of the graphene layers.[28] In addition, the nearly identical I_D/I_G values between GO and FGO nanosheets indicate that the covalent bonding occurs between the polymer chains and GO sheets without significant destruction of the carbon lattice.

The changes between GO and FGO were characterized by XRD curves in **Figure 5b**. The diffraction pattern of GO includes a sharp peak (001) at a low diffraction angle of 2θ = 10.5°, which corresponds to a d-spacing of 0.766 nm. The phenomenon indicates the presence of large amounts of oxygen-containing groups and water molecules trapped between the GO nanosheets. The XRD pattern of FGO nanosheets exhibits an intensive peak (001) at 6.7°, which corresponds to the interlayer d-space of 1.373 nm. Also, a less-intense diffraction peak (002) can be seen at 2θ = 20.5°, which is related to the amorphous structure of the L-HAR grafted onto the surface of GO. The increase in d-spacing values can be attributed to the L-HAR moieties bonding to the GO surface.

Figure 5c presents UV–vis spectra of GO and FGO dispersed in water. For GO, it exhibits two characteristic features: an intensive peak at 200 nm, which corresponds to π-π^* transitions of aromatic C=C bonds.[25] While for FGO, the results show that its π-π^* transitions of aromatic C=C bonds have shifted to 197 nm. Besides, the board peak at around 230 nm being assigned to the acrylic resin indicates that the L-HAR has been grafted onto the GO surface successfully.

Figure 5d presents the TGA curves of the GO and FGO nanosheets under nitrogen. For the former, its weight loss in the range 20–170 °C can be attributed to the evaporation of the absorbed water between layers of the nanosheets, while a significant decomposition that starts at approximately 180 °C is likely due to the pyrolysis of the unstable oxygen-containing species (such as the hydroxyl, carbonyl, and carboxylic groups), which generates gases including CO, CO_2, and steam.[26] While for the latter, the grafted polymer chains can inhibit the

absorption of water, so its weight loss at 20–170 °C is relatively low. However, as the heat-resistant property of acrylic resins is relatively worse than GO, it decomposes completely when the temperature increased beyond 500 °C, so the amount of residual FGO is relatively less than the pure GO.

3.2 Composite coatings of HAD doped with GO/FGO nanosheets

The effect of the doped GO or FGO on the properties of composite coatings was studied. At first, the size and zeta-potential of the obtained GO-d-HAD and FGO-d-HAD samples were tested. All the samples present a relatively uniform particle size distribution (PDI < 0.1). Besides, all the zeta-potential is at around –55 mV, suggesting that the doped GO or FGO has no detectable effect on the dispersion stability of HAD during its storage time. Also, the particle size of HAD is increased with the doped GO or FGO due to the dispersion effect. When DI water was added, the doped GO or FGO nanosheets act as the inorganic dispersing agent to pack more water-dispersible polymer resins and form the aqueous hydroxy acrylic acid dispersion with a bigger size during the phase-inversion process. As FGO presents more compatibility with the organic compounds, the obtained FGO-d-HAD shows a larger particle size.[27]

Table 2: Particle size and zeta-potential of HAD and GO or FGO-doped HAD

Sample	Particle size (nm)	PDI	Zeta-potential (mV)
Pure HAD	78.79	0.065	–55.37
GO-d-HAD	101.02	0.014	–53.12
FGO-d-HAD	139.59	0.054	–55.28

To cure the HAD samples, the isocyanate curing agent, Aquolin®268 was added and the mixtures were coated onto the glass or tinned plate and cured at room temperature.

Some studies reported that the coatings doped with GO have an excellent elastic modulus of 250 GPa.[28] Thus, the effects of doped GO or FGO on the mechanical properties of the dried composite coatings were studied by tensile test. The stress-strain curves of the different coatings and the corresponded tensile parameters obtained from these curves are shown in **Figure 6**. FGO-d-HAD coating demonstrates an increase of the stress and strain at the break, by an order of 70 % and 92 %, respectively, when compared to the original HAD coating. While, for GO-d-HAD coating, it presents relatively poor mechanical properties, i.e., the doped GO might degrade the mechanical property of the cured composite coating. This could be from the nanoscale spaces in the coatings, which are created during the curing process due to the poor compatibility between the doped GO and polymer resins. However, when the GO nanosheets are functionalized by L-HAR, their dispersibility in the HAD matrix can increase the interlayer space of nanosheets, which will overcome the van der Waals forces between the GO sheets and lead to a decrease in the surface hydrophilicity and also less agglomeration occurs in the case of the FGO-d-HAD coatings.[29] The interface of the FGO nanosheets and the cured HAD interface is completely different from that of the bulk of the HAD. The FGO nanosheets may provide many stress-damping sites in the cured coatings. The bonding at the FGO nanosheets/HAD interface is mostly linear rather than a more cross-linked structure of the bulk of HAD. So the FGO-d-HAD interface would be more flex-

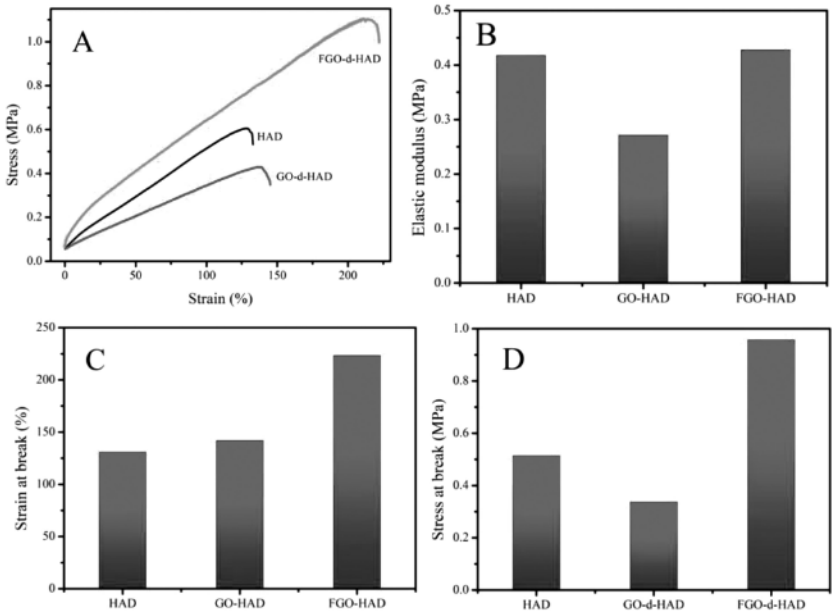

Figure 6: Tensile and flexural properties of pure HAD and its nanocomposites: A) stress-strain curves, B) elastic modulus, C) elongation at the break, D) stress at break

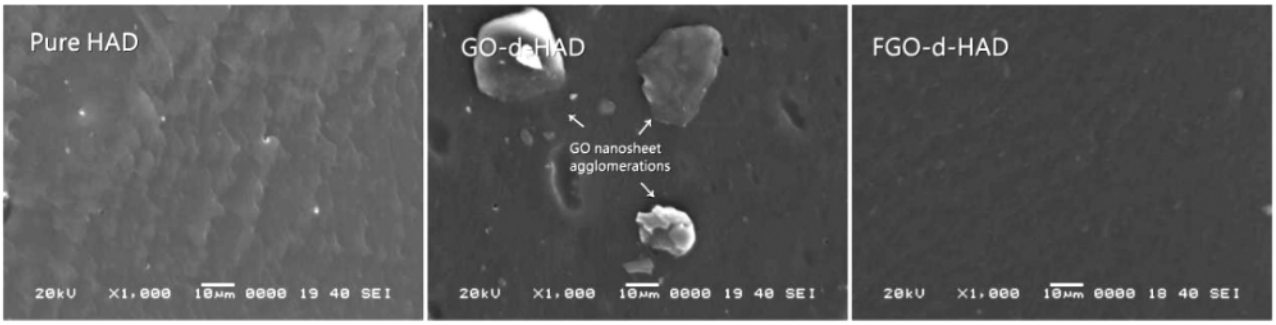

Figure 7: SEM micrographs from the cross-section of the pure HAD, GO-d-HAD, and FGO-d-HAD samples after tensile test

ible and can easily dissipate the transferred stress without destruction. The presence of numerous interfaces in the FGO-d-HAD coating will lead to optimization of the HAD matrix tensile strength property.

The effect of these nanosheets on the fracture-surface morphology of the dried coating was further investigated via SEM analysis. **Figure 7** shows that the tensile fractured surface of pure HAD is relatively rough with cracks and ruptured areas, indicating poor stress damping and crack-deflection properties of the cured coating. In the case of GO nanosheets, the agglomeration is obvious at some parts of the fractured surface. Conversely, it is obvious that the surfaces of FGO-d-HAD coatings are comparatively more smooth, and no agglomeration can be seen. This means that most of the FGO nanosheets were well dispersed in the HAD matrix. The observed morphologies are in agreement with the tensile-test results. The improved dispersion and bonding of the FGO nanosheets are responsible for the appearance of the fracture at the interface of the FGO/HAD rather than in the bulk phase.[30] The energy dissipation during deformation occurs at the FGO/HAD interface and increases the roughness with no crack progress at the fracture surface after the tensile test.[31]

Table 3 summarizes the mechanical properties of the cured coatings. When GO is doped into the pure HAD,

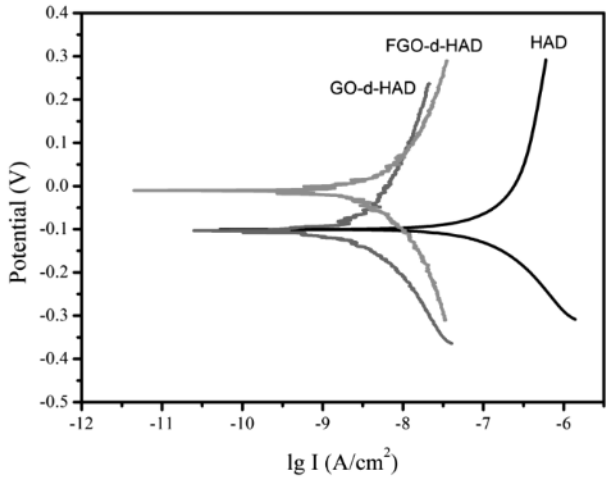

Figure 8: Polarization curves of HAD, GO-d-HAD, and FGO-d-HAD coatings

pencil hardness is enhanced, which may be attributed to the accumulated GO nanosheets in the dried coating.[32] However, the aggregated GO can also affect the interior flexibility and adhesion properties of the cured GO-d-HAD coatings. Fortunately, the FGO-d-HAD-based coating has better mechanical properties, possibly because of the good dispersion of the FGO nanosheets in the HAD matrix benefits to improve the mechanical properties of the cured coatings. The dispersion behaviors of the GO or FGO nanosheets may have a tremendous impact on the mechanical properties of the dried coatings.

Table 3: Mechanical properties of the self-crosslinkable fluorescent coatings

Samples	Pencil Hardness	Flexibility	Adhesion
Pure HAD	2B	1 mm	0
GO-d-HAD	HB	3 mm	2
FGO-d-HAD	HB	1 mm	0

To explore the effect of GO or FGO on the anti-corrosion property of the cured coating, the electrochemical corrosion test such as potentiodynamic polarization curves was performed by soaking the coatings in 3.5 % NaCl solution (**Figure 8**). The potentials (E_{corr}) and corrosion-current densities (I_{corr}) are calculated by Tafel extrapolation, and the values are listed in **Table 4**.

Table 4: Electrochemical parameters of the coatings obtained from the potentiodynamic polarization test

Samples	E_{corr} and I_{corr} of the dried coatings	
	E_{corr} (I = 0) (V)	I_{corr} (A/cm^2)
HAD	–0.10018	1.5579×10^{-7}
GO-d-HAD	–0.15361	6.847×10^{-9}
FGO-d-HAD	–0.010235	9.5546×10^{-9}

Compared with the pure HAD coating, I_{corr} values of GO-d-HAD and FGO-d-HAD are smaller, which indicates that the corrosion rate of the HAD coating can be reduced by doping GO or FGO nanosheet. However, only the E_{corr} value of the FGO-d-HAD shifts to a more positive position, which indicates its better corrosion-protection property. It can be explained that the grafting of GO with L-HAR significantly enhances the

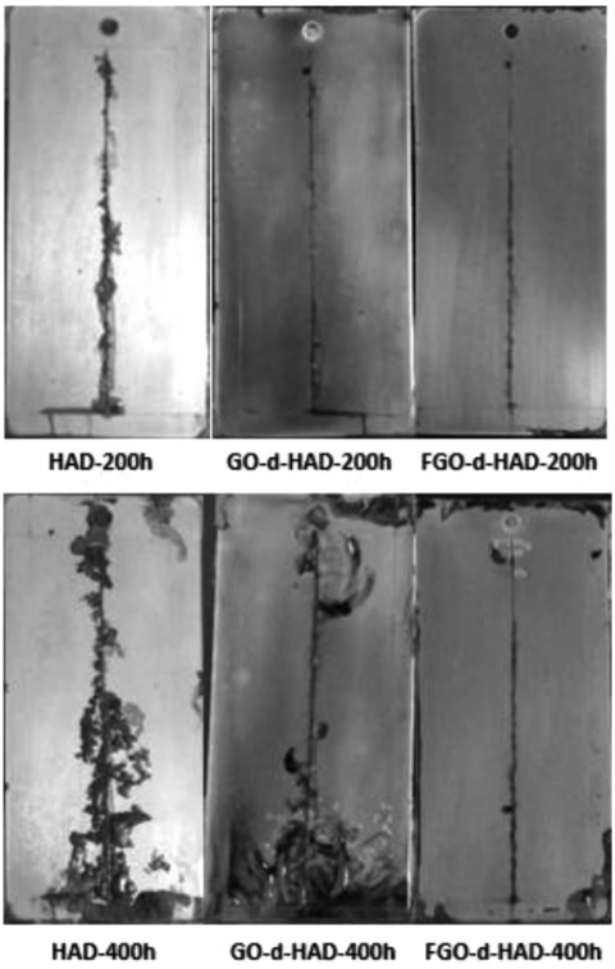

Figure 9: Visual performances of HAD, GO-d-HAD, and FGO/HAD coatings exposed to salt-spray test for 200 h and 400 h

interfacial compatibility and combination between GO and the HAD matrix, which is beneficial for reducing the defects of the coating and increasing the barrier property of the GO nanosheets in the cured composite coatings.[35]

Various coatings were exposed to salt-spray tests to evaluate their corrosion resistance. **Figure 9** depicts the visual performance of the coatings after 200 h and 400 h, respectively. It clearly shows that the corrosion products are significantly produced around scribes of the original HAD coating, which indicates poor corrosion resistance. Doping of the GO or FGO into the HAD coating caused a visual decrease in the number of corrosion products around the scribes of the coating. In particular, it can be seen that the coatings with the FGO dopants resulted in the least amount of corrosion products created around the scribes. A larger disbonding area of the HAD and GO-d-HAD coatings after being exposed to the salt-spray test confirms that the FGO nanosheets are capable of enhancing the corrosion resistance of the dried coating. In addition, doping FGO into the HAD coating enhances the performance of the coating's corrosion protection better than GO-d-HAD and pure HAD coatings.

4 CONCLUSIONS

Aqueous hydroxy acrylic acid dispersions (HAD) doped with GO and functionalized/hydroxylated acrylic resin grafted GO(FGO) were prepared. Various characterizations demonstrated that the hydroxylated acrylic resin was successfully grafted onto the surface of the GO nanosheets. TEM and SEM analyses revealed that such hydroxylated acrylic resin functionalization of GO changed its dispersion behavior, which could benefit the interfacial interaction with the GO nanosheet and acrylate resin matrix and provided ameliorating effects in the improvement of mechanical and anti-corrosion properties of the FGO-d-HAD composite coatings. This work paves a new way to functionalize GO and its application into the waterborne resins to enhance the properties of the cured coatings.

Acknowledgments

This work was funded by the National Key Laboratory for Marine Coatings (Grant No. GZ-19-0001) and the National Natural Science Foundation of China (Grant No. 51673088)

5 REFERENCES

[1] G. Cui, Z. X. Bi, S. H. Wang, J. G. Liu, X. Xing, Z. L. Li, B. Y. Wang, A comprehensive review on smart anti-corrosive coatings, Prog Org Coat., 148 (**2020**), 105821, doi:10.1016/j.porgcoat.2020.105821

[2] W. Li, Z. Qiu, M. Tebyetekerwa, J. Zhang, Y. Wang, T. Gao, J. Wang, Y. Ding, Y. Xie, Preparation of silica/polymer nanocomposites with aggregation-induced emission properties as fluorescent responsive coatings, Prog Org Coat., 127 (**2019**) 8–15, doi:10.1016/j.porgcoat.2018.11.001

[3] W. Yao, M. Tebyetekerwa, X. Bian, W. Li, S. Yang, M. Zhu, R. Hu, Z. Wang, A. Qin, B. Z. Tang, Materials interaction in aggregation-induced emission (AIE)-based fluorescent resin for smart coatings, J Mater Chem C., 6 (**2018**) 47, 12849–12857, doi:10.1039/C8TC04175J

[4] W. Li, D. Huang, X. Xing, J. Tang, Y. Xing, X. Li, J. Zhang, Study the factors affecting the performance of organic–inorganic hybrid coatings, J Appl Polym Sci., 131 (**2014**) 21, doi:10.1002/app.41010

[5] F. Zhang, W. Liu, L. Liang, S. Wang, H. Shi, Y. Xie, M. Yang, K. Pi, The effect of functional graphene oxide nanoparticles on corrosion resistance of waterborne polyurethane, Colloids and Surfaces A: Physicochemical and Engineering Aspects, 591 (**2020**), 124565, doi:10.1016/j.colsurfa.2020.124565

[6] W. Li, J. Wang, Y. Xie, M. Tebyetekerwa, Z. Qiu, J. Tang, S. Yang, M. Zhu, Z. Xu, Water-based fluorescent paint: Presenting a novel approach to study and solve the aggregation caused quench (ACQ) effect in traditional fluorescent materials, Prog Org Coat., 120 (**2018**), 1–9, doi:10.1016/j.porgcoat.2018.03.003

[7] M. Kim, Y. Kim, S. H. Baeck, S. E. Shim, Effect of surface treatment of graphene nanoplatelets for improvement of thermal and electrical properties of epoxy composites, Carbon Lett., 16 (**2015**) 1, 34–40, doi:10.5714/CL.2015.16.1.034

[8] Y. Du, N. Li, T. L. Zhang, Q. P. Feng, Q. Du, X. H. Wu, G. W. Huang, Reduced graphene oxide coating with anticorrosion and electrochemical property-enhancing effects applied in hydrogen storage system, ACS Appl Mater Inter., 9 (**2017**) 34, 28980–28989, doi:10.1021/acsami.7b05809

[9] B. Ramezanzadeh, E. Ghasemi, M. Mahdavian, E. Changizi, M. M. Moghadam, Characterization of covalently-grafted polyisocyanate chains onto graphene oxide for polyurethane composites with improved mechanical properties, Chem Eng J., 281 (**2015**), 869–883, doi:10.1016/j.cej.2015.07.027

[10] Y. Ma, H. Di, Z. Yu, L. Liang, L. Lv, Y. Pan, Y. Zhang, D. Yin, Fabrication of silica-decorated graphene oxide nanohybrids and the properties of composite epoxy coatings research, Appl Surf Sci., 360 (**2016**), 936–945, doi:10.1016/j.apsusc.2015.11.088

[11] H. C. Schniepp, J. L. Li, M. J. McAllister, H. Sai, M. Herrera-Alonso, D. H. Adamson, R. K. Prud'homme, R. Car, D. A. Saville, I. A. Aksay, Functionalized single graphene sheets derived from splitting graphite oxide, J Phys Chem B., 110 (**2006**) 17, 8535–8539, doi:10.1021/jp060936f

[12] K. H. Liao, Y. Qian, C. W. Macosko, Ultralow percolation graphene/polyurethane acrylate nanocomposites, Polymer, 53 (**2012**) 17, 3756–3761, doi: 10.1016/j.polymer.2012.06.020

[13] L. Hu, P. Jiang, P. Zhang, G. Bian, S. Sheng, M. Huang, Y. Bao, J. Xia, Amine-graphene oxide/waterborne polyurethane nanocomposites: effects of different amine modifiers on physical properties, J Mater Sci., 51 (**2016**) 18, 8296-8309, doi:10.1007/s10853-016-9993-5

[14] D. Song, Z. Yin, F. Liu, H. Wan, J. Gao, D. Zhang, X. Li, Effect of carbon nanotubes on the corrosion resistance of water-borne acrylic coatings, Prog Org Coat., 110 (**2017**), 182–186, doi:10.1016/j.porgcoat.2017.04.043

[15] D. A. Dikin, S. Stankovich, E. J. Zimney, R. D. Piner, G. H. Dommett, G. Evmenenko, S. T. Nguyen, R. S. Ruoff, Preparation and characterization of graphene oxide paper, Nature, 448 (**2007**), 7152, 457–460, doi:10.1038/nature06016

[16] B. Ramezanzadeh, M. M. Moghadam, N. Shohani, M. Mahdavian, Effects of highly crystalline and conductive polyaniline/graphene oxide composites on the corrosion protection performance of a zinc-rich epoxy coating, Chem Eng J., 320 (**2017**), 363–375, doi:10.1016/j.cej.2017.03.061

[17] D. Hou, M. Han, Y. Muhammad, Y. Liu, F. Zhang, Y. Yin, S. Duan, J. Li, Performance evaluation of modified asphalt based trackless tack coat materials, Construction and Building Materials, 165 (**2018**), 385–394, doi:10.1016/j.conbuildmat.2017.12.187

[18] S. K. Yadav, J. W. Cho, Functionalized graphene nanoplatelets for enhanced mechanical and thermal properties of polyurethane nanocomposites, Appl Surf Sci., 266 (**2013**), 360–367, doi:10.1016/j.apsusc.2012.12.028

[19] W. Li, D. Huang, J. Wang, W. Shen, L. Chen, S. Yang, M. Zhu, B. Tang, G. Liang, Z. Xu, A novel stimuli-responsive fluorescent elastomer based on an AIE mechanism, Polymer Chemistry, 6 (**2015**) 47, 8194–8202, doi:10.1039/C5PY01273B

[20] M. G. Sari, M. Shamshiri, B. Ramezanzadeh, Fabricating an epoxy composite coating with enhanced corrosion resistance through impregnation of functionalized graphene oxide-co-montmorillonite Nanoplatelet, Corrosion Science, 129 (**2017**), 38–53, doi:10.1016/j.corsci.2017.09.024

[21] J. Liang, Y. Huang, L. Zhang, Y. Wang, Y. Ma, T. Guo, Y. Chen, Molecular©Ðlevel dispersion of graphene into poly (vinyl alcohol) and effective reinforcement of their nanocomposites, Advanced Functional Materials, 19 (**2009**) 14, 2297–2302, doi:10.1002/adfm.200801776

[22] Y. Hu, C. Liu, Q. Shang, Y. Zhou, Synthesis and characterization of novel renewable castor oil-based UV-curable polyfunctional polyurethane acrylate, Journal of Coatings Technology and Research, 15 (**2018**) 1, 77–85, doi:10.1007/s11998-017-9948-z

[23] N. Parhizkar, T. Shahrabi, B. Ramezanzadeh, A new approach for enhancement of the corrosion protection properties and interfacial adhesion bonds between the epoxy coating and steel substrate through surface treatment by covalently modified amino functionalized graphene oxide film, Corrosion science, 123 (**2017**), 55–75, doi:10.1016/j.corsci.2017.04.011

[24] R. B. Vignesh, J. Balaji, M. Sethuraman, Surface modification, characterization and corrosion protection of 1, 3-diphenylthiourea doped sol-gel coating on aluminium, Prog Org Coat., 111 (**2017**), 112–123, doi:10.1016/j.porgcoat.2017.05.013

[25] N. Yousefi, M. M. Gudarzi, Q. Zheng, X. Lin, X. Shen, J. Jia, F. Sharif, J.-K. Kim, Highly aligned, ultralarge-size reduced graphene oxide/polyurethane nanocomposites: mechanical properties and moisture permeability, Composites Part A: Applied Science and Manufacturing, 49 (**2013**), 42–50, doi:10.1016/j.compositesa.2013.02.005

[26] W. Li, W. Shen, W. Yao, J. Tang, J. Xu, L. Jin, J. Zhang, Z. Xu, A novel acrylate-PDMS composite latex with controlled phase compatibility prepared by emulsion polymerization, Journal of Coatings Technology and Research, 14 (**2017**) 6, 1259–1269, doi:10.1007/s11998-017-9923-8

[27] H. Zheng, M. Guo, Y. Shao, Y. Wang, B. Liu, G. Meng, Graphene oxide–poly (urea–formaldehyde) composites for corrosion protection of mild steel, Corrosion Science, 139 (**2018**), 1–12, doi:10.1016/j.corsci.2018.04.036

[28] L. C. Tang, Y. J. Wan, D. Yan, Y. B. Pei, L. Zhao, Y. B. Li, L. B. Wu, J. X. Jiang, G. Q. Lai, The effect of graphene dispersion on the mechanical properties of graphene/epoxy composites, Carbon, 60 (**2013**), 16–27, doi:10.1016/j.carbon.2013.03.050

[29] Q. Li, C. Liu, J. Wen, Y. Wu, Y. Shan, J. Liao, The design, mechanism and biomedical application of self-healing hydrogels, Chinese Chemical Letters, 28 (**2017**) 9, 1857–1874, doi:10.1016/j.cclet.2017.05.007

[30] Y. Pottathara, S. Thomas, N. Kalarikkal, T. Grießer, Y. Grohens, V. Bobnar, M. Finšgar, V. Kokol, R. Kargl, UV-Induced reduction of graphene oxide in cellulose nanofibril composites, New journal of chemistry, 43 (**2019**) 2, 681–688, doi:10.1039/C8NJ03563F

[31] P. Haghdadeh, M. Ghaffari, B. Ramezanzadeh, G. Bahlakeh, M. R. Saeb, The role of functionalized graphene oxide on the mechanical and anti-corrosion properties of polyurethane coating, Journal of the Taiwan Institute of Chemical Engineers, 86 (**2018**), 199–212, doi:10.1016/j.jtice.2018.02.009

[32] W. Chen, P. Liu, L. Min, Y. Zhou, Y. Liu, Q. Wang, W. Duan, Non-covalently functionalized graphene oxide-based coating to enhance thermal stability and flame retardancy of PVA film, Nano-micro letters, 10 (**2018**) 3, 1–13